



저작자표시-비영리-변경금지 2.0 대한민국

이용자는 아래의 조건을 따르는 경우에 한하여 자유롭게

- 이 저작물을 복제, 배포, 전송, 전시, 공연 및 방송할 수 있습니다.

다음과 같은 조건을 따라야 합니다:



저작자표시. 귀하는 원저작자를 표시하여야 합니다.



비영리. 귀하는 이 저작물을 영리 목적으로 이용할 수 없습니다.



변경금지. 귀하는 이 저작물을 개작, 변형 또는 가공할 수 없습니다.

- 귀하는, 이 저작물의 재이용이나 배포의 경우, 이 저작물에 적용된 이용허락조건을 명확하게 나타내어야 합니다.
- 저작권자로부터 별도의 허가를 받으면 이러한 조건들은 적용되지 않습니다.

저작권법에 따른 이용자의 권리는 위의 내용에 의하여 영향을 받지 않습니다.

이것은 [이용허락규약\(Legal Code\)](#)을 이해하기 쉽게 요약한 것입니다.

[Disclaimer](#)

Integrin  $\beta$ 4-mediated metabolic  
reprogramming of  
cancer-associated fibroblasts  
in triple negative breast cancer

Jin Sol Sung

Department of Medical Science

The Graduate School, Yonsei University

Integrin  $\beta$ 4-mediated metabolic  
reprogramming of  
cancer-associated fibroblasts  
in triple negative breast cancer

Jin Sol Sung

Department of Medical Science

The Graduate School, Yonsei University

Integrin  $\beta$ 4-mediated metabolic  
reprogramming of  
cancer-associated fibroblasts  
in triple negative breast cancer

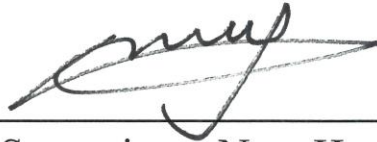
Directed by Professor Nam Hoon Cho

The Doctoral Dissertation  
submitted to the Department of Medical Science,  
the Graduate School of Yonsei University  
in partial fulfillment of the requirements for the degree of  
Doctor of Philosophy of Medical Science

Jin Sol Sung

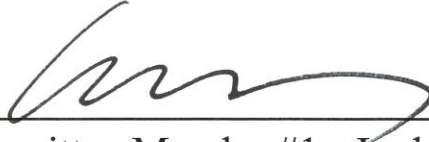
June 2019

This certifies that the Doctoral Dissertation of  
Jin Sol Sung is approved.



---

Thesis Supervisor : Nam Hoon Cho



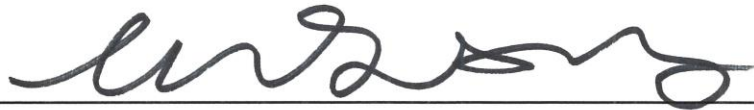
---

Thesis Committee Member#1 : Joohyuk Sohn



---

Thesis Committee Member#2 : Jae Ho Cheong



---

Thesis Committee Member#3 : Ja Seung Koo



---

Thesis Committee Member#4 : Young Chan Chae

The Graduate School  
Yonsei University

June 2019

## **ACKNOWLEDGEMENTS**

Firstly, I would like to give my sincere gratitude to my advisor Prof. Nam Hoon Cho for the support of my Ph.D study and related research, for his patience, motivation, and immense knowledge. He took time out to hear, guide and keep me on the correct path to complete this research. I could not have imagined having a better advisor and mentor for my Ph.D study.

Besides my advisor, I would like to thank the rest of my thesis committee: Prof. Joohyuk Sohn, Prof. Jae Ho Cheong, Prof. Ja Seung Koo and Prof. Young Chan Chae for their insightful comments and encouragement, but also for the hard question which incited me to widen my research from various perspectives.

My thanks also go out to my fellow labmates Dr. Baek Gil Kim, Dr. Yeosue Jang and Ms. Suki Kang for their contributions to the direction and richness of this research. Without their support it would never have taken shape.

Lastly, I extend my deepest thanks to my family: my husband, and my parents and parents in laws, and to my brother and my sister in law for supporting me spiritually and keeping all circumstances in favor to me throughout writing this thesis.

## TABLE OF CONTENTS

ABSTRACT.....	1
I. INTRODUCTION .....	3
II. MATERIALS AND METHODS .....	6
1. Human fibroblasts isolation and cell cultures .....	6
2. Real-time PCR analysis.....	7
3. Genetic manipulation .....	8
4. Western blot analysis .....	8
5. Lactate assay.....	9
6. Migration matrigel assay .....	10
7. Exosome isolation.....	10
8. Apoptosis detection assay.....	11
9. Glucose uptake assay .....	11
10. Flow cytometry analysis .....	11
11. Xenograft mouse model .....	12
12. Transmission electron microscopic analysis.....	12
13. Confocal imaging .....	13
14. Luciferase assay .....	14
15. Statistical analysis.....	14
III. RESULTS .....	15
1. Integrin $\beta$ 4-overexpressing TNBC cells increased integrin $\beta$ 4 protein level in cancer-associated fibroblasts via exosome transfer .....	15

2. Cancer-derived exosomal integrin $\beta 4$ transfer increased glycolysis in cancer-associated fibroblasts .....	19
3. Integrin $\beta 4$ -dependent glycolysis was associated with mitochondrial fission and clearance .....	22
4. Integrin $\beta 4$ overexpression induced BNIP3L-dependent mitophagy in cancer-associated fibroblasts .....	27
5. Integrin $\beta 4$ -dependent reverse Warburg effect contributes to breast cancer progression .....	31
6. Schematic design .....	36
7. The expression of integrin $\alpha 6$ in the CAFs co-cultured with or without breast cancer cell lines .....	37
8. The fluorescence microscopic images of the mouse tumor tissues .....	37
9. Primers for real-time PCR analysis .....	38
IV. DISCUSSION .....	39
V. CONCLUSION .....	42
REFERENCES .....	43
ABSTRACT (IN KOREAN) .....	50
PUBLICATION LIST .....	52

## LIST OF FIGURES

Figure 1. TNBC-specific integrin $\beta 4$ expression in CAFs .....	16
Figure 2. TNBC cells transfer integrin $\beta 4$ protein to CAFs via exosome.....	18
Figure 3. Exosomal integrin $\beta 4$ induces glycolysis in CAFs .....	20
Figure 4. Exosomal integrin $\beta 4$ regulates glycolysis-related gene expression in CAFs .....	21
Figure 5. Glycolytic CAFs promote mitochondrial fragmentation .....	23
Figure 6. Integrin $\beta 4$ -induced mitochondrial fission leads to mitophagy in CAFs .....	24
Figure 7. Integrin $\beta 4$ -overexpressing CAFs facilitate damaged mitochondria clearance .....	26
Figure 8. Integrin $\beta 4$ directly regulates BNIP3L by c-Jun activation in CAFs .....	28
Figure 9. Integrin $\beta 4$ -overexpressing CAFs undergo autophagy through AMPK activation .....	30
Figure 10. Integrin $\beta 4$ -dependent reverse Warburg effect contributes to breast cancer progression .....	33
Figure 11. Exosomal integrin $\beta 4$ promotes tumor growth and angiogenesis <i>in vivo</i> .....	35
Figure 12. Integrin $\beta 4$ -mediated metabolic reprogramming of cancer-associated fibroblasts in triple negative breast cancer .....	36

Supplementary Figure S1. The expression of integrin  $\alpha 6$  in the  
CAFs co-cultured with or without breast  
cancer cell lines ..... 37

Supplementary Figure S2. The fluorescence microscopic  
images of the mouse tumor tissues..... 37

## **LIST OF TABLES**

Supplementary Table S1. Primers for real-time PCR analysis  
..... 38

ABSTRACT

**Integrin  $\beta$ 4-mediated metabolic reprogramming of  
cancer-associated fibroblasts in triple negative breast cancer**

Jin Sol Sung

*Department of Medical Science  
The Graduate School, Yonsei University*

(Directed by Professor Nam Hoon Cho)

New therapeutic strategies are urgently required for triple-negative breast cancer (TNBC), as few targeted therapies are currently available. Targeting the tumor microenvironment is a novel approach that may prove beneficial for TNBC patients. In this study, we found that TNBC-specific integrin  $\beta$ 4 expression and its extracellular release via exosomes led to its uptake by cancer-associated fibroblasts (CAFs). Blockade of exosomal integrin  $\beta$ 4 secretion by MDA-MB-231 cells lowered its uptake by CAFs. Exosomal integrin  $\beta$ 4 uptake by CAFs induced lactate production and glycolysis-related gene expression. Moreover, integrin  $\beta$ 4-induced glycolytic stress elevated the rates of mitochondrial fission, which in turn stimulated mitophagy to preserve mitochondrial quality. BCL2 interacting protein 3 like (BNIP3L) expression was upregulated by integrin  $\beta$ 4-mediated c-Jun activation.

Integrin  $\beta$ 4-overexpression in CAFs increased microtubule associated protein 1 light chain 3 (LC3) levels and stimulated autophagosome formation. Excess lactate production by integrin  $\beta$ 4-overexpressing CAFs induced TNBC proliferation and invasion by upregulating the expression of monocarboxylate transporter 1 (MCT1). In a xenograft experiment, exosomal integrin  $\beta$ 4 promoted tumor growth and angiogenesis. Collectively, these results demonstrate that integrin  $\beta$ 4 uptake in CAFs via exosomal transfer induces aerobic glycolysis, which results in excess lactate production and promotes TNBC cell proliferation and invasion as well as tumor growth and angiogenesis.

---

Key words : integrin  $\beta$ 4, mitophagy, reverse Warburg effect

**Integrin  $\beta$ 4-mediated metabolic reprogramming of  
cancer-associated fibroblasts in triple negative breast cancer**

Jin Sol Sung

*Department of Medical Science  
The Graduate School, Yonsei University*

(Directed by Professor Nam Hoon Cho)

**I. INTRODUCTION**

There is a lack of promising therapeutic strategies for triple-negative breast cancers (TNBCs), as they lack the expression of validated breast cancer therapeutic targets like estrogen (ER), progesterone (PR), and herceptin 2 receptor (Her2). Therefore, targeting stromal cells, such as fibroblasts, is being considered as a potential therapeutic strategy against TNBC<sup>1-3</sup>. The importance of stromal cells within the tumor microenvironment is well accepted, as these cells play an important role in determining cancer cell behavior and clinical outcomes<sup>4,5</sup>. Cancer-associated fibroblasts (CAFs), the major population of tumor

stromal cells, have been identified by expression profiling to predict clinical prognosis in breast cancer patients, independent of other factors<sup>6,7</sup>. Therefore, understanding the biological role of CAFs is required for further insight into TNBC progression.

Integrin  $\alpha6\beta4$  is a heterodimeric transmembrane receptor that binds to laminin-332 in the extracellular matrix (ECM). As integrin  $\beta4$  only pairs with integrin  $\alpha6$ , integrin  $\beta4$  expression can be used as a proxy to measure integrin  $\alpha6\beta4$  expression<sup>8</sup>. The latter complex plays an important role in signal transduction by relaying signals from the extracellular matrix to the cell interior. Emerging studies suggest that integrin  $\beta4$  contributes to tumor progression in various cancers such as lung, ovarian, bladder, and breast cancer<sup>9-11</sup>. Indeed, high levels of integrin  $\beta4$  expression are associated with poor prognosis and facilitate the migration, invasion, and survival of TNBC cells<sup>12-14</sup>.

Exosomes are small vesicles that play important roles in cancer progression. These vesicles are secreted by various cells and contain functional biomolecules such as proteins, lipids, RNA, and DNA. With respect to cancer, cell-derived exosomal proteins are transferred to recipient cells within the tumor microenvironment establishing a malignant phenotype and promoting cancer cell invasion and migration. Interestingly, a recent study indicated that exosomal integrin  $\beta4$  derived from breast cancer cells is involved in organ-specific metastasis<sup>15,16</sup>.

CAFs affect adjacent epithelial tumor cells by partaking in growth factor secretion, ECM remodeling and tumor immunity; all of which promote cancer progression<sup>4,17-19</sup>. Moreover, work by Pavlides has indicated that CAFs play a key role in cancer cell metabolism, resulting higher proliferative capacity of cancer cells. CAFs rely on the reverse Warburg effect, whereby these cells utilize aerobic glycolysis for energy, resulting in increased secretion of lactate that is exported by monocarboxylated transporter 4 (MCT4) present on the CAF membranes. This lactate can then be taken up by the lactate importer MCT1 present in cancer cells and used as fuel. Several studies have suggested that CAFs with altered metabolism induce breast tumorigenesis<sup>20-22</sup>. Increased metabolic stress in CAFs triggers mitochondrial fragmentation and degradation<sup>23</sup>. Depending on the severity, this increased metabolic stress may even lead to apoptosis<sup>23,24</sup>. Under conditions where the mitochondria become dysfunctional, AMP-activated protein kinase (AMPK) is activated that restores energy homeostasis, to maintain mitochondrial function and eliminate damaged mitochondria via mitophagy<sup>25-28</sup>.

The aim of this study is to investigate the contribution of integrin  $\beta$ 4 overexpression in CAFs to TNBC progression. Integrin  $\beta$ 4 may be acquired by CAFs from TNBC cell-derived exosomes. Our study implicates the potential use of exosomal integrin  $\beta$ 4 as a therapeutic target in TNBC.

## **II. MATERIALS AND METHODS**

### **1. Human fibroblast isolation and cell cultures**

Cancer associated fibroblasts (CAFs) were isolated from the breast cancer patients undergoing surgery at Severance Hospital of the Yonsei University Health System, South Korea. The research protocol was approved by the Severance Hospital Ethics Committee (IRB number 4-2008-0383). All patients were informed of tissue use of comprehensive experiments and signed consent forms. To isolate CAFs, tissue was cut into small pieces, placed in a digestion solution of enzyme cocktail (ISU ABXIS, Seoul, South Korea), and incubated in a humidified incubator at 37°C and 5% CO<sub>2</sub> overnight. The digested cell mixture was filtered through a 70 µm cell strainer (BD Bioscience, Franklin Lakes, NJ) and then centrifuged at 485 x g for 5 min. The resulting pellet was resuspended with medium, added into the Ficoll (Histopaque®-1077, sigma, 1.077 g/ml), and centrifuged at 90 x g for 2 min. The supernatant containing fibroblasts was further centrifuged at 485 x g for 9 min. The final pellet was resuspended with the Dulbecco's Modified Eagle Medium: Nutrient Mixture F-12 (DMEM/F12, Gibco BRL, Grand island, NY) containing 20% fetal bovine serum (FBS; Gibco BRL, Grand island, NY) supplemented with 100 IU/ml penicillin, 100 µg/ml streptomycin (Gibco BRL, Grand island, NY), and then placed in a humidified incubator containing 5% CO<sub>2</sub> at 37°C. The fibroblastic characteristics of the isolated cells were determined by both microscopic morphology and immunostaining with antibodies

against vimentin (Abcam, Cambridge, UK), cytokeratin (Dako, Glostrup, Denmark) and cytokeratin 5 (Novocastra Newcastle upon Tyne, UK). Breast cancer cell lines (MDA-MB-231, BT-20, MDA-MB-453, MCF7, BT-474, and SK-BR-3 cells) were purchased from the Korean Cell Line Bank (authenticated using morphology and STR profiling) and cultured with the DMEM (Gibco BRL, Grand island, NY) containing 10% FBS (Gibco BRL, Grand island, NY) supplemented with 100 IU/ml penicillin, 100 µg/ml streptomycin (Gibco BRL, Grand island, NY) under the same experimental conditions as the fibroblasts. For co-culture, CAFs were incubated with the serum-free DMEM/F12 containing 5 µM CellTracker Green CMFDA (5-chloromethylfluorescein diacetate; Invitrogen, Carlsbad, CA) dye at 37°C for 30 min, washed with phosphate buffered saline (PBS, Gibco BRL, Grand island, NY), and added with a fresh medium. Unstained cancer cells were seeded onto the CMFDA-stained CAFs, and then cultured with serum-reduced DMEM/F12 (0.5% FBS) for 1 day.

## **2. Real-time PCR analysis**

Total RNA was extracted using TRIzol (Invitrogen, Carlsbad, CA) and quantitated by NanoDrop Spectrophotometer (ThermoFisher Scientific, Waltham, MA). For cDNA synthesis, 1 µg of total RNA was reverse-transcribed using Hyperscript™ First strand synthesis kit (Geneall, Seoul, Korea) in a PTC-200 Thermal Cycler (MJ Research, Reno, NV, USA). For quantitative analysis, 25 ng of the resulting cDNA was amplified in a

CFX Connect™ Real-Time PCR Detection System (Bio-Rad Laboratories; Hercules, CA, USA) using LaboPass™ SYBR Green Q Master (Cosmogenetech, Seoul, South Korea). The PCR experiments were performed in triplicated, and relative expression values were calculated according to the  $\Delta\Delta C_t$  method. All primer sequences were provided in Supplemental table S1.

### **3. Genetic manipulation**

For a transient gene overexpression, CAFs were seeded into 6-well plate to reach 80% confluence. Plasmid vectors (empty, integrin  $\alpha_6$ , integrin  $\beta_4$ , or pQCXI Puro DsRed-LC3-GFP) were transfected into the CAFs using Lipofectamine® LTX with Plus™ and then incubated for 48 hr. pQCXI Puro DsRed-LC3-GFP was a gift from David Sabatini (Addgene plasmid #31182 ; <http://n2t.net/addgene:31182> ; RRID:Addgene\_31182) <sup>21</sup>. To establish an integrin  $\beta_4$  knockdown MDA-MB-231 cells, MDA-MB-231 cells were transduced with lentivirus containing integrin  $\beta_4$  shRNA.

### **4. Western blot analysis**

Protein extracts were prepared by cell lysis with a PRO-PREP™ kit (iNtRON biotechnology, Seongnam-si, South Korea) and centrifuged at  $15,000 \times g$  for 15 min using Centrifuge 5810R (Eppendorf, Hamburg, Germany). The protein concentration of the

resulting supernatant was measured using the Bradford protein assay kit (Bio-Rad, Hercules, CA). 20 µg protein was electrophoresed on 10% polyacrylamide gels in Tris/glycine (Invitrogen®, Carlsbad, CA), transferred to a polyvinylidene difluoride (PVDF) membrane (Millipore Corporation, Billerica, MA), and then probed with primary antibodies against LAMC2, Integrin  $\alpha$ 6, Integrin  $\beta$ 4, GAPDH, ACTB, CD63, PINK1, PRKN, BNIP3, BNIP3L, JNK, p-JNK, c-Jun, p-c-Jun, AMPK, FIS1 (Santa Cruz Biotechnology, Dallas, TX), OPA1, MFN1, DRP1, DRP1(Ser616), DRP1(Ser637) (Cell signaling technology, Danvers, MA), ULK1 (Invitrogen, Carlsbad, CA), LDHA, LDHB, MCT4, p-AMPK, and LC3 (Abcam; Cambridge, UK). The blotted membrane was blocked with 0.5% BSA at RT for 1 h and then followed by incubation with HRP-tagged secondary antibodies against mouse, rabbit (GenDEPOT, Barker, TX) or goat (Invitrogen, Carlsbad, CA). Immunoreactive bands were visualized by enhanced chemiluminescence (ECL) detection kit (GenDEPOT, Barker, TX).

## **5. Lactate assay**

The amount of lactate in cell lysate and supernatant was measured using Lactate assay kit (Biovision, Milpitas, CA) according to manufacturer's instructions. Briefly, 50 µl of sample was mixed with 50 µl of the master reaction mix containing 46 µl of lactate assay buffer, 2 µl of lactate enzyme mix, and 2 µl of lactate probe in a well of a 96-well plate. 30 min after incubation, absorbance was measured in at 570 nm using Spectramax plus 96/384 (MTX

Lab Systems, Bradenton, FL, USA). Lactate amount was measured in triplicate, calculated using the standard curve prepared with known concentration of lactate, and then normalized with protein concentration.

## **6. Migration matrigel assay**

CAFs and MDA-MB-231 cells were seeded to lower chamber and matrigel-coated transwell insert respectively, and then placed in a humidified incubator at 37°C and 5% CO<sub>2</sub> for 24 hr. After incubation, non-invading cells were removed from the upper surface of the matrigel by scrubbing. The invaded cells to the lower surface of the matrigel was stained with 0.1% crystal violet, and rinsed with distilled water. The dried matrigel was placed on a slide, added with a drop of immersion oil, and then covered with a coverslip.

## **7. Exosome isolation**

CMs were collected from cancer cells and centrifuged at 3000 x g for 15 min. The resulting supernatant was transferred to a new tube, mixed with the appropriate volume of ExoQuick-TC (SBI, Palo Alto, CA), incubated at 4°C for 24hr, and then was centrifuged at 1500 x g for 30 min. Supernatant was aspirated and then the mixture was centrifuged at 1500 x g for 5 min to remove residual supernatant. The exosome pellet was resuspended to use or stored at -20°C.

## **8. Apoptosis detection assay**

Apoptosis was analyzed using Annexin V-FITC detection kit (BD Bioscience, Franklin Lakes, NJ) according to the manufacturer's instructions. Briefly, CAFs were washed twice with cold PBS, centrifuged, and then resuspended with binding buffer at a concentration of  $1 \times 10^6$  cells/ml. 100  $\mu$ l of the cell suspension was mixed with 5  $\mu$ l of Annexin V-FITC and PI. 15 min after incubation in the dark at room temperature, the mixture was added with 400  $\mu$ l of binding buffer and then analyzed using FACSVerse (BD Bioscience, Franklin Lakes, NJ).

## **9. Glucose uptake assay**

Glucose uptake was measured using Glucose Uptake Glo kit (Promega, Madison, WI) according to the manufacturer's instructions. CAFs ( $1.5 \times 10^4$ ) were seeded in a well of 96-well plate and placed for 24 hr. The CAFs were washed with glucose-free PBS and incubated with 2DG (1 mM) for 10 min. Stop and Neutralization buffer were added to the well and mixed one by one. 2DG6P detection reagent was added to the CAFs and then incubated at RT for 30 min. Glucose uptake was measured using luminometer (EG & G Berthold, Bad Wildbad, Germany) in triplicate.

## **10. Flow cytometry analysis**

Cells ( $0.5 \times 10^6$ ) was washed with 1 ml of the PBS containing 2% FBS (2% FBS-PBS) and

then centrifuged at 150 x g for 3min. After removing supernatant, the resulting cell pellet was resuspended with 50  $\mu$ l of the 2% FBS-PBS containing primary antibody and incubated at 4°C for 1 hr. After resuspending and centrifugation, cell pellet was incubated in the dark with 100  $\mu$ l of FITC or PE-conjugated secondary antibody (Santa Cruz Biotechnology, Dallas, TX) in the same way as the primary antibody. After washing, the cell pellet was resuspended with 500  $\mu$ l of 2% FBS-PBS, and then analyzed by FACSVerse (BD Bioscience, Franklin Lakes, NJ).

### **11. Xenograft mouse model**

GFP-overexpressing CAFs ( $3 \times 10^6$ ) were subcutaneously co-transplanted to six-week-old BALB/c Nude mice with RFP-overexpressing MDA-MB-231 or RFP-overexpressing integrin  $\beta 4$  knockdown MDA-MB-231 cells ( $1 \times 10^6$ ) using Matrigel (Invitrogen, Carlsbad, CA). Tumor size (length and width) was measured every 3 days using calipers for one month. The volume of tumor mass was calculated using the formula:  $V = (W \times W \times L)$ , where W is the width and L is the length.

### **12. Transmission electron microscopic analysis**

CAFs transfected with control or integrin  $\beta 4$  plasmid were harvested with trypsin-EDTA (Gibco BRL, Grand island, NY), placed to 1.5 ml tube, and immediately fixed with 4%

paraformaldehyde at RT for 30 min. After washing three times with PBS by centrifugation at 300 x g for 5 min, the CAFs were embedded in 100% Eponate resin (Ted Pella Inc, Redding, CA) at 60°C for 24 hr. 1- $\mu$ m-thick sections were cut using an ultramicrotome (Leica, Wetzlar, Germany), stained with 2% aqueous uranyl acetate for 15 min, rinsed with distilled water, and then stained with lead citrate (Leica, Wetzlar, Germany). The stained sections were examined on JEM1011 transmission electron microscope (JEOL, Tokyo, Japan).

### **13. Confocal imaging**

CAFs were fixed with 4% paraformaldehyde at 4°C for 15 min and then permeabilized with 1% Triton X-100 (Sigma-Aldrich, St. Louis, Mo) at RT for 10 min. After being washed twice with PBST, the CAFs were blocked with 1% BSA at RT for 1hr and then incubated with primary antibodies against integrin  $\beta$ 4 and CD63 (Santa Cruz Biotechnology, Dallas, TX) at 4°C overnight. Following to washing, fluorescence-conjugated secondary antibodies against mouse (Santa Cruz Biotechnology, Dallas, TX) were added to the CAFs and incubated at RT for 1hr. The CAFs were washed, added with a drop of mounting solution (Abcam, Cambridge, UK), covered with a coverslip, and then analyzed with with LSM700 laser scanning confocal microscope (Carl Zeiss, Oberkochen, Germany).

#### **14. Luciferase assay**

The putative c-Jun binding sites were analyzed in the 2kb upstream sequences of human *BNIP3L* gene using PROMO<sup>38</sup>. Three putative binding sites on *BNIP3L* were amplified from the genomic DNA of CAFs using conventional PCR. Deletion mutants were constructed from the PCR products by an overlap extension PCR method<sup>39</sup>. The wild-type and deletion mutant constructs were cloned into pGL3 vector. For dual luciferase assays, each cloned plasmid was co-transfected with pRL-TK in HEK293T ( $2 \times 10^5$ ) cells using Lipofectamine® LTX with Plus™ Reagent (Invitrogen®, Carlsbad, CA, USA). 48 hr after transfection, luciferase activity was measured from the cell lysates using a dual-luciferase reporter assay system (Promega; Madison, WI, USA).

#### **15. Statistical analysis**

Statistical significance was determined using t-test and anova (two-tailed). The results were considered to be significant at  $p < 0.05$ . All statistical analyses were performed using Prism 6 for Windows (GraphPad Software, Inc.; La Jolla, CA, USA). Asterisks indicate p values: one for  $p < 0.05$ , two for  $p < 0.01$ , and three for  $p < 0.001$ .

### III. RESULTS

Immunohistochemical staining was performed to assess the expression of integrin  $\beta$ 4 in each breast cancer subtype. Integrin  $\beta$ 4 expression was significantly higher in TNBC patients than non-TNBC patients (Figure 1A). In addition, integrin  $\beta$ 4 was specifically expressed in the CAFs of TNBC patients. Consistent with this result, integrin  $\beta$ 4 expression in TNBC cells, and in CAFs co-cultured with TNBC cells was also upregulated *in vitro* (Figure 1B and C). Since integrin  $\beta$ 4 expression can be induced by the soluble factors secreted from MDA-MB-231 and BT-20, CAFs were stimulated with the conditioned medium (CM) from MDA-MB-231, BT-20, and Hs578T (negative control) cells. However, integrin  $\beta$ 4 expression was not induced by the CM from any of TNBC cells (Figure 1D).

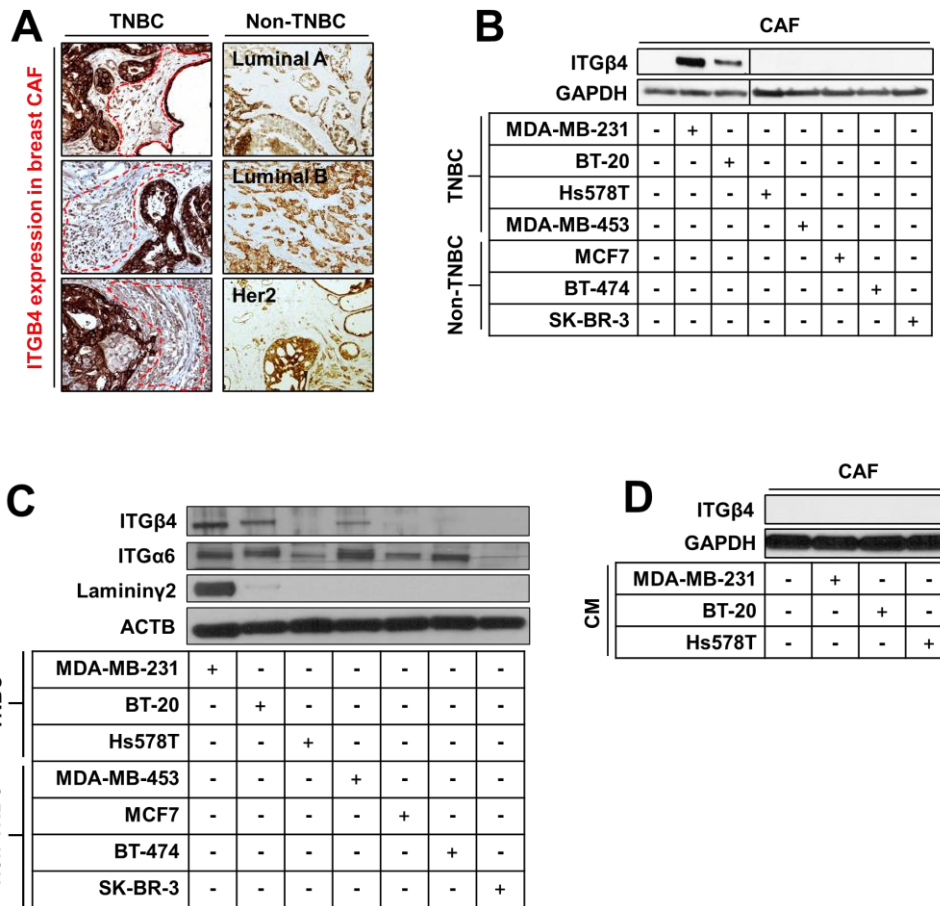


**Figure 1. TNBC-specific integrin  $\beta 4$  expression in CAFs.** Integrin  $\beta 4$  overexpression in (A) TNBC stroma using the patient tumor tissues and (B) CAFs co-cultured with TNBC cells. Integrin  $\beta 4$  expression in (C) breast cancer cell lines and (D) CAFs stimulated with CMs from breast cancer cells.

We next investigated the mechanism of expression of integrin  $\beta$ 4 in CAFs. Previous studies have indicated that tumor-derived exosomal integrin  $\beta$ 4 uptake in distant CAFs contributes to metastasis<sup>15</sup>. As shown in Figure 2A, integrin  $\beta$ 4 was present abundantly in exosomes derived from the TNBC cell line MDA-MB-231, compared to those derived from other TNBC cell lines, BT-20 and Hs578T. Integrin  $\beta$ 4 and CD63 (an exosome marker) were weakly co-localized in the CAFs cultured with MDA-MB-231 cells (control) in the transwell co-culture system, however they were not co-localized in the CAFs cultured with integrin  $\beta$ 4 knockdown MDA-MB-231 cells (Figure 2B). Although CD63 was detected in the CAFs co-cultured with integrin  $\beta$ 4 knockdown MDA-MB-231 cells, integrin  $\beta$ 4 expression was not detected. Similarly, in the transwell co-culture system, integrin  $\beta$ 4 and CD63 were strongly co-localized in the CAFs cultured with MDA-MB-231 cells (control), however they were not co-localized in the CAFs cultured with integrin  $\beta$ 4 knockdown MDA-MB-231 cells (Figure 2C). To further evaluate exosomal integrin  $\beta$ 4 transfer, MDA-MB-231 cells were pretreated with GW4869 (10  $\mu$ M, an exosome inhibitor) for 2 days, and then cultured with CAFs in a direct co-culture system. As shown in Figure 2D, the co-localization of integrin  $\beta$ 4 and CD63 was dramatically reduced in the CAFs cultured with GW4869-treated MDA-MB-231 cells. Integrin  $\beta$ 4 protein expression was strongly detected in the CAFs co-cultured with MDA-MB-231 cells, but not in those co-cultured with integrin  $\beta$ 4 knockdown MDA-MB-231 cells (Figure 2E) and GW4869-treated MDA-MB-231 cells (Figure 2F).

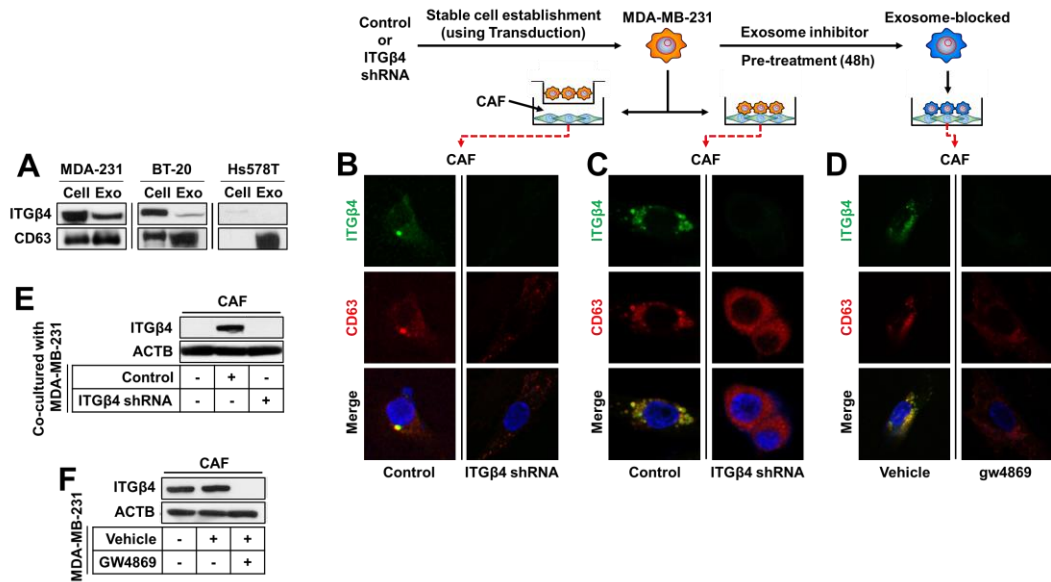


**Figure 2. TNBC cells transfer integrin  $\beta 4$  protein to CAFs via exosome.** (A) Integrin  $\beta 4$  expression in TNBC cells and -derived exosomes. TNBC-derived integrin  $\beta 4$  transfer to CAFs in (B) a transwell co-culture and (C) a direct co-culture. (D) Exosome-mediated integrin  $\beta 4$  transfer in the direct co-culture. MDA-MB-231 cells were pretreated with 10  $\mu\text{M}$  of GW4869 for 48h. Integrin  $\beta 4$  expression in (E) the direct co-culture and (F) the direct co-culture with or without GW4869. To establish stable integrin  $\beta 4$  knockdown cancer cells, MDA-MB-231 cells were transduced with the lentivirus containing control (empty) or integrin  $\beta 4$  shRNA. To block the exosomal transfer of integrin  $\beta 4$ , MDA-MB-231 cells were pretreated with GW4869 for 1day.

To investigate the role of integrin  $\beta 4$  expression on metabolic shift in CAFs (from oxidative phosphorylation to glycolysis), we measured lactate production<sup>29</sup>. Uptake of exosomal integrin  $\beta 4$  by CAFs elevated their lactate production (Figure 3A). A similar response was also observed in whole cell lysate of CAFs that overexpressed integrin  $\beta 4$  (Figure 3B) and its CM (Figure 3C), however the effect was inhibited by integrin  $\beta 4$  knockdown (Figure 3D) and pre-treatment with GW4869, an exosome inhibitor (Figure 3E). Further, glucose uptake also increased in CAFs that overexpressed integrin  $\beta 4$  (Figure 3F).

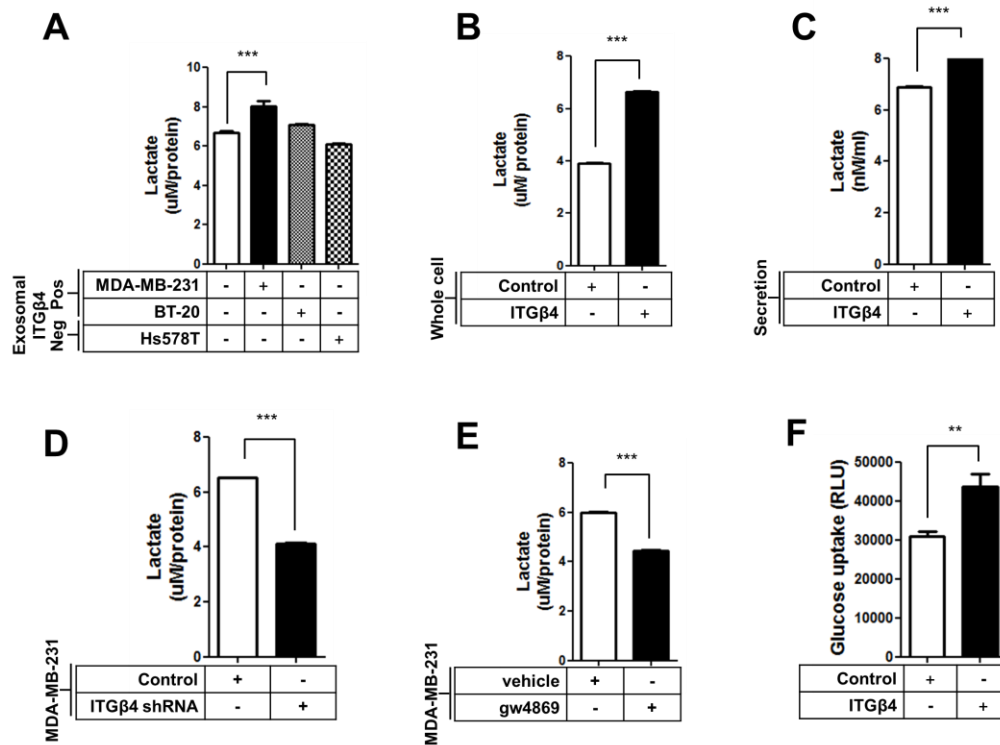


**Figure 3. Exosomal integrin  $\beta 4$  induces glycolysis in CAFs.** Lactate production in (A) CAFs co-cultured with TNBC cells, (B) whole lysate of CAFs transfected with integrin  $\beta 4$  plasmids, (C) CM of CAFs transfected with integrin  $\beta 4$  plasmids, (D) CAFs co-cultured with integrin  $\beta 4$  knockdown MDA-MB-231 cells, and (E) CAFs co-cultured with MDA-MB-231 pretreated with GW4869 for 1 day. (F) Glucose uptake in integrin  $\beta 4$ -overexpressing CAFs. Co-culture was performed in the transwell co-culture. The membrane pore size of transwell insert was  $0.4 \mu\text{m}$ .

Consistent with these results, an increased expression of lactate dehydrogenase A (LDHA, which converts pyruvate to lactate) was observed upon the uptake of integrin  $\beta 4$  by CAFs from MDA-MB-231-derived exosomes and also upon the overexpression of integrin  $\beta 4$  in CAFs (Figure 4). In contrast, the expression of lactate dehydrogenase B (LDHB, showing antagonistic effect to LDHA) remained unchanged in integrin  $\beta 4$ -overexpressing CAFs. MCT4 expression was downregulated in CAFs upon the uptake of integrin  $\beta 4$  from MDA-MB-231-derived exosomes but was upregulated in integrin  $\beta 4$ -overexpressing CAFs (Figure 4). These observations suggest that integrin  $\beta 4$  expression in CAFs is involved in aerobic glycolysis, even in the presence of oxygen.

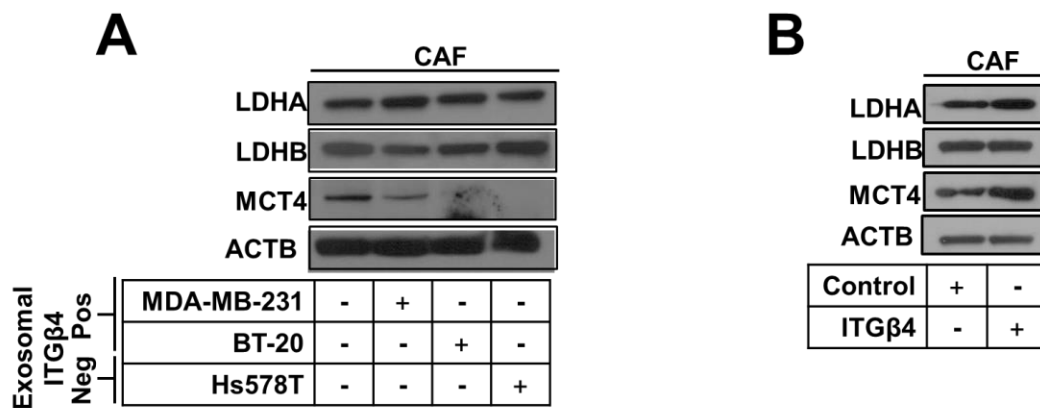


**Figure 4. Exosomal integrin  $\beta 4$  regulates glycolysis-related gene expression in CAFs.**

The expression of glycolysis-related genes in (A) CAFs co-cultured with TNBC cells and (B) integrin  $\beta 4$ -overexpressing CAFs.

Mitochondrial fission significantly increases in response to high levels of glycolytic stress, while mitochondrial fusion concomitantly decreases<sup>30-32</sup>. Mitochondrial dynamin like ATPase (Opa1) and mitofusin1 (Mfn1) proteins, essential for mitochondrial fusion, were downregulated upon integrin  $\beta$ 4-overexpression (Figure 5A). In contrast, expressions of mitochondrial fission 1 protein (Fis1), dynamin-1-like protein (Drp1), and phosphorylation of Drp1(Ser616), which have critical roles in mitochondrial fission, were upregulated in integrin  $\beta$ 4-overexpressing CAFs, suggesting increased mitochondrial fission (Figure 5B). Transmission electron microscopy (TEM) was performed to visualize mitochondrial morphology. Consistent with the expression levels of mitochondrial proteins, we observed a higher rate of mitochondrial fission in integrin  $\beta$ 4-overexpressing CAFs than in control CAFs (Figure 5C).

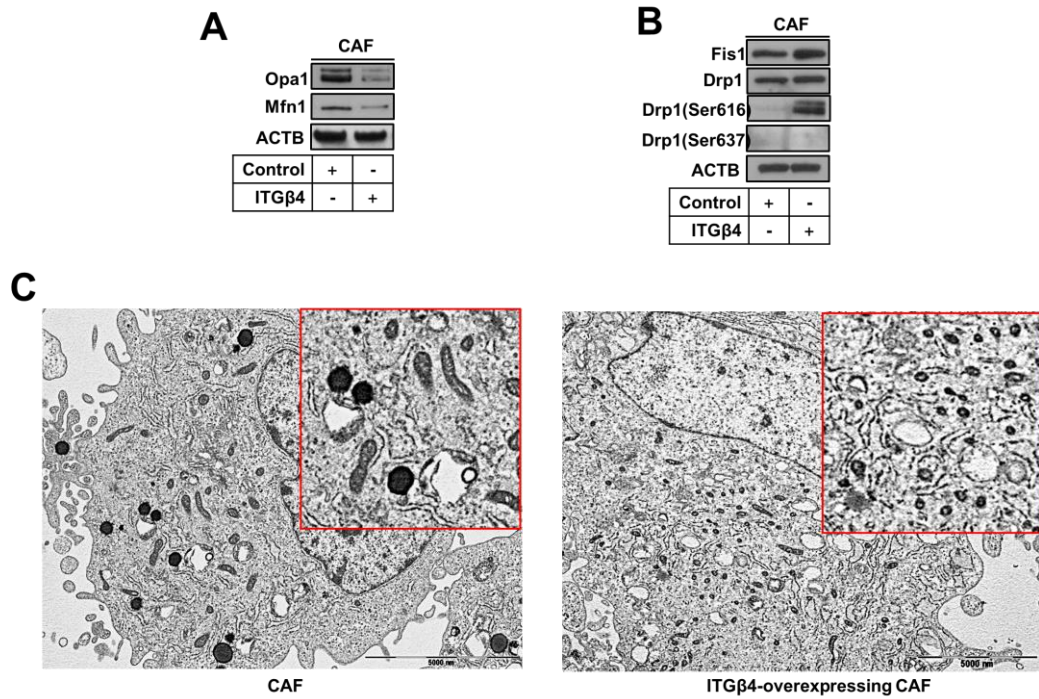


**Figure 5. Glycolytic CAFs promote mitochondria fragmentation.** The expression of mitochondrial (A) fusion and (B) fission-related genes. (C) The transmission electron microscopic image of integrin  $\beta$ 4-induced mitochondrial fission.

Mitochondrial fission facilitates mitophagy and promotes the recruitment of BCL2 interacting protein 3 like (BNIP3L) to that is essential for mitochondrial clearance<sup>33-35</sup>. Here, we found that BNIP3L was upregulated in integrin  $\beta$ 4-overexpressing CAFs, reflected by an increase in mitophagy (Figure 6A). However, no change in expression was detected in PTEN-induced kinase1/parkin (PINK/PARKIN), suggesting that integrin  $\beta$ 4-mediated mitophagy in CAFs is related to BNIP3L. Indeed, immunofluorescence analyses indicated that integrin  $\beta$ 4-positive CAFs co-expressed BNIP3L (Figure 6B).

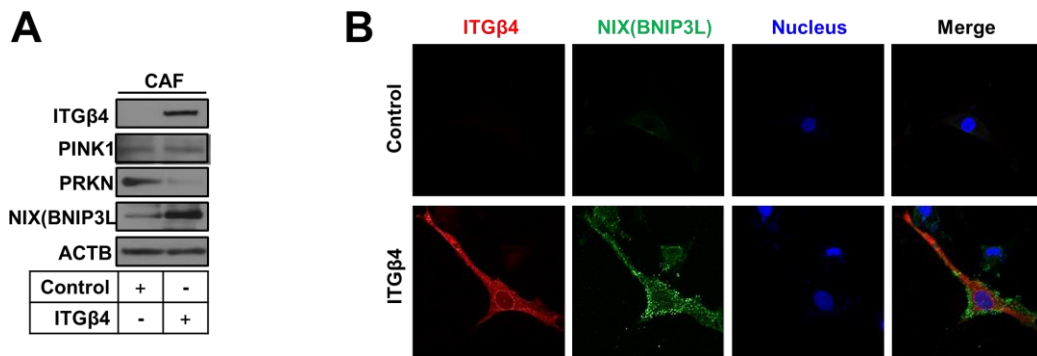


**Figure 6. Integrin  $\beta$ 4-induced mitochondrial fission leads to mitophagy in CAFs.**

(A) The expression of mitophagy-related factors in the integrin  $\beta$ 4-overexpressing CAFs.

(B) The fluorescent microscopic image of integrin  $\beta$ 4-induced BNIP3L overexpression in CAFs.

We further confirmed the occurrence of mitophagy using TEM. Strikingly, a large population of mitochondria was observed enclosed within double-membraned autophagosomes, in integrin  $\beta$ 4-overexpressing CAFs compared to control CAFs (Figure 7A). To test the prevalence of mitophagy upon integrin  $\beta$ 4 overexpression, annexin V staining was performed. However, no significant change in cell death was observed between control cells and CAFs overexpressing integrin  $\beta$ 4 (Figure 7B).

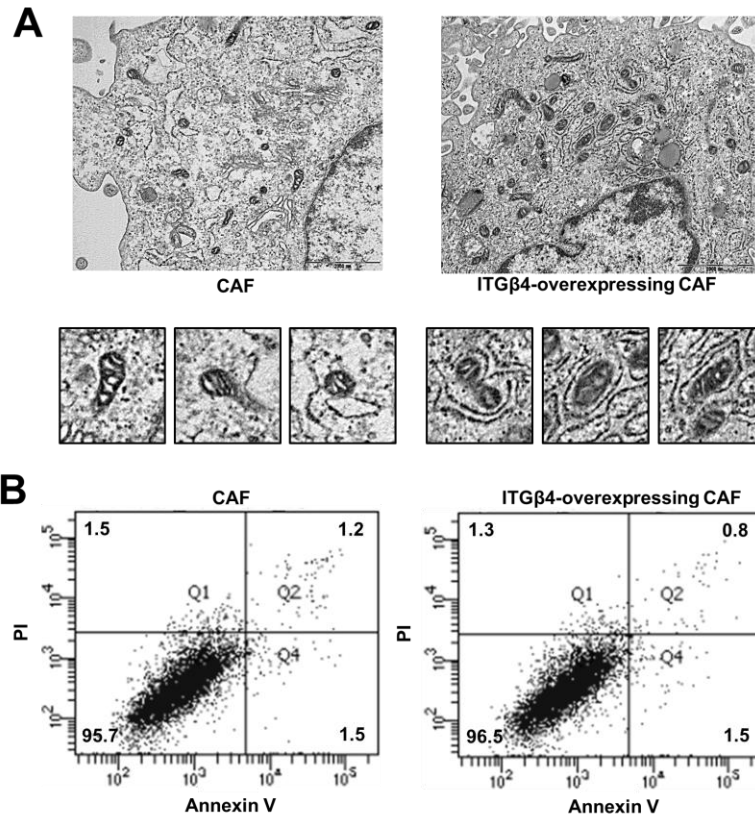


**Figure 7. Integrin  $\beta$ 4-overexpressing CAFs facilitate damaged mitochondria clearance.** (A) The transmission electron microscopic image of integrin  $\beta$ 4-induced mitochondrial clearance. (B) Cell viability comparison between wild-type and integrin  $\beta$ 4-overexpressing CAFs.

As BNIP3L was strongly upregulated upon integrin  $\beta$ 4 overexpression in CAFs, we sought to examine the direct role of integrin  $\beta$ 4 in BNIP3L regulation. To this end, the upstream 2 kb sequence of the BNIP3L promoter region was analyzed using a transcription prediction program (TFSEARCH). Through this program, we identified that the putative transcription factor c-Jun was capable of binding the queried 2 kb promoter sequence of BNIP3L. We generated three c-Jun deletion mutants within specific binding sites; and assessed the binding affinities of wild-type c-Jun and the three mutants to the 2 kb promoter sequence, using a dual luciferase assay (Figure 8A, left). The luciferase activity was significantly higher in the assay with wild-type c-Jun as compared to c-Jun that contained a mutation in the first binding site (-13 bp to -7 bp, TCAGTC) (Figure 8A, right). No significant difference was observed between wild-type and deletion mutants for the other binding sites. Thus, integrin  $\beta$ 4 could potentially activate BNIP3L transcription via the transcription factor c-Jun. To further confirm if integrin  $\beta$ 4 directly regulates BNIP3L through c-Jun activation, we determined the levels of phosphorylated (activated) c-Jun and its upstream kinase – c-Jun N-terminal kinase (JNK). Phosphorylated c-Jun and JNK were both upregulated in integrin  $\beta$ 4-overexpressing CAFs (Figure 8B). Interestingly, BNIP3L expression was suppressed in integrin  $\beta$ 4-overexpressing CAFs in the presence of sp600124, an inhibitor of c-Jun (Figure 8C).

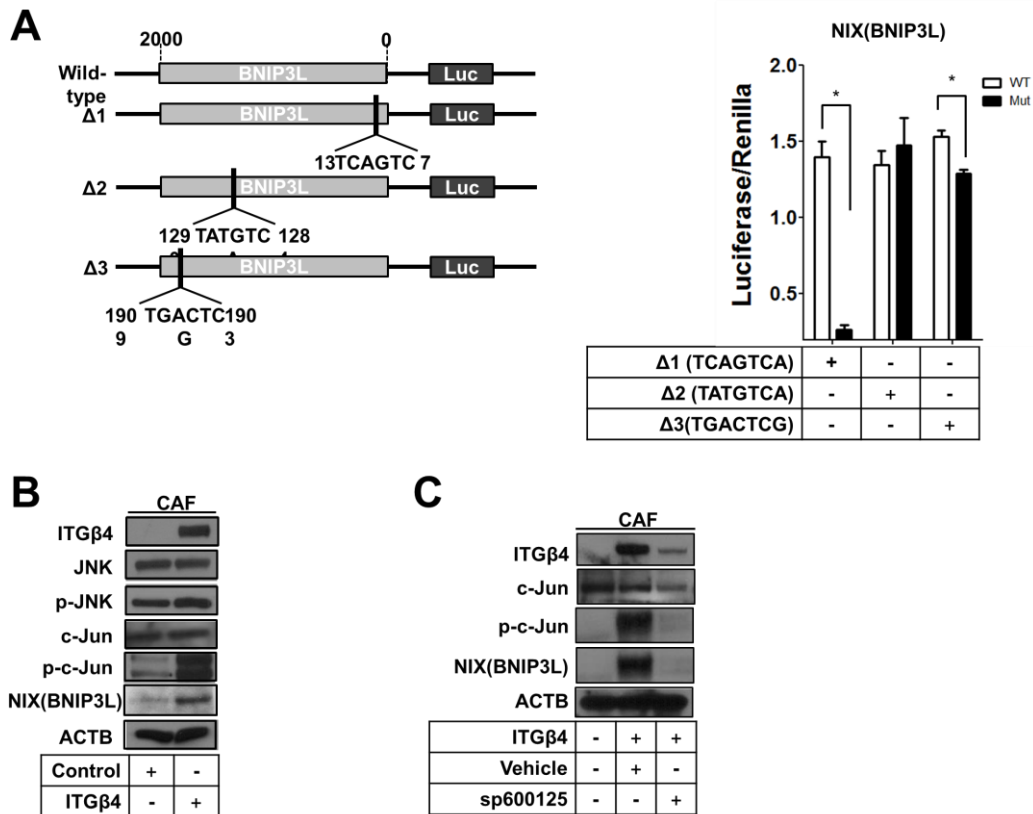


**Figure 8. Integrin  $\beta 4$  directly regulates BNIP3L by c-Jun activation in CAFs.** (A) Dual luciferase reporter assay. The wild-type or mutant sequences of putative c-Jun binding sites on BNIP3L were cloned into pGL3 vector. c-Jun binding to BNIP3L was examined by dual luciferase assay. (B) Integrin  $\beta 4$ -dependent mitophagy signaling pathway in CAFs. (C) The suppression of integrin  $\beta 4$ -dependent mitophagy signaling in CAFs by JNK inhibitor.

Emerging evidences suggest that BNIP3L-dependent mitophagy is capable of recruiting the autophagy machinery to the mitochondria. Further, BNIP3L directly interacts with the microtubule associated protein 1 light chain 3 (LC3)<sup>36-40</sup>. Autophagy activation is regulated by the AMP-activated protein kinase (AMPK). Phosphorylation of AMPK promotes autophagy and activates unc-51 like autophagy activating kinase 1 (ULK1), which inhibits the autophagic cascade<sup>41,42</sup>. In this study, AMPK phosphorylation was upregulated in integrin  $\beta$ 4-overexpressing CAFs (Figure 9A). Further, ULK1 and LC3-II expression levels exhibited similar trends of upregulation (Figure 9A). To visualize autophagosome formation, we used GFP-LC3B-DsRed whose GFP tag is degraded during autophagosome formation. The number of DsRed-LC3 puncta increased in integrin  $\beta$ 4-overexpressing CAFs suggesting an increase in autophagosome formation (Figure 9B). Since BNIP3L is known to directly bind LC3, we next visualized the co-localization of BNIP3L and LC3, marked by GFP and RFP, respectively. Compared to the control CAFs, co-localization between BNIP3L and LC3 was higher in integrin  $\beta$ 4-overexpressing CAFs (Figure 9C). Taken together, these data imply that integrin  $\beta$ 4-induced mitophagy facilitates damaged mitochondrial clearance by entering the autophagic pathway, but acts independently of autophagic cell death.

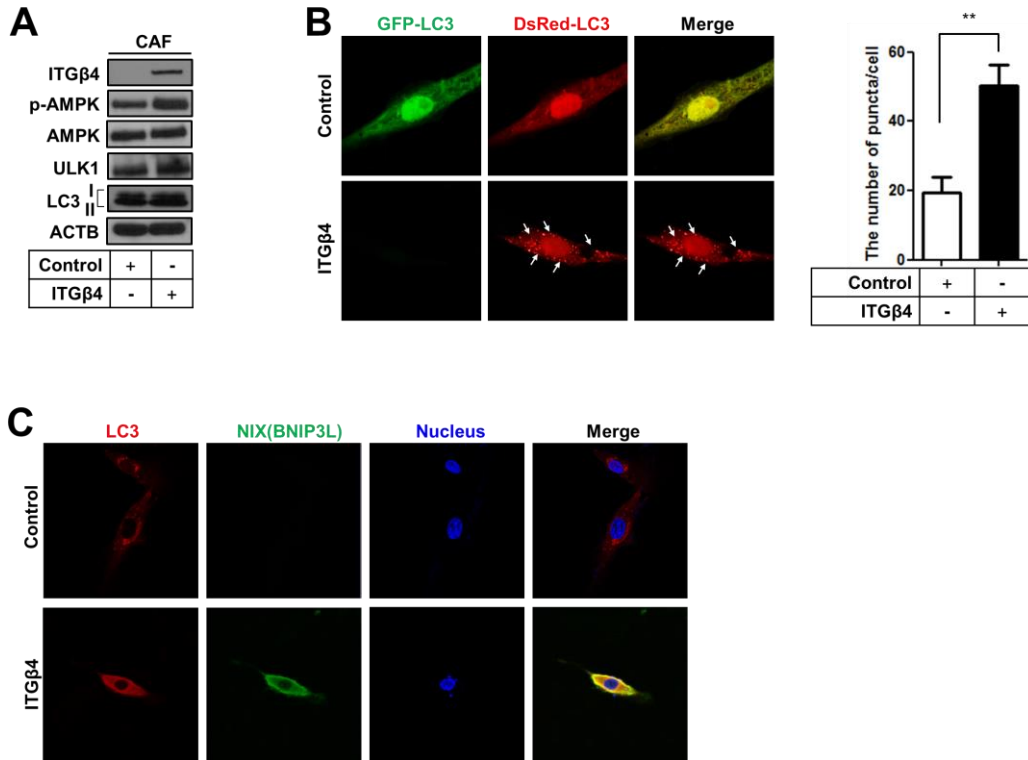


**Figure 9. Integrin  $\beta$ 4-overexpressing CAFs undergo autophagy through AMPK activation.** (A) Integrin  $\beta$ 4-induced autophagy signaling in CAFs. (B) Puncta formation in integrin  $\beta$ 4-overexpressing CAFs. For a puncta formation assay, pOCXI puro DsRed-LC3-GFP was transfected into CAFs. (C) Co-localization between LC3 and BNIP3L in integrin  $\beta$ 4-overexpressing CAFs.

Since integrin  $\beta 4$  plays a role in regulation of glycolysis in CAFs, we next set out to determine the effect of integrin  $\beta 4$  overexpressing CAFs on TNBC cells. We first investigated the level of membrane localized MCT1 in MDA-MB-231 cells to test whether MDA-MB-231 cells uptake lactate as an energy source through MCT1. Interestingly, MDA-MB-231 incubated with conditioned medium (CM) from integrin  $\beta 4$ -overexpressing CAFs demonstrated significantly higher levels of MCT1, compared to those grown in CM from control CAFs (Figure 10A). Next, a proliferation assay was used to assess MDA-MB-231 cell proliferation. CM from integrin  $\beta 4$ -overexpressing CAFs strikingly accelerated the growth of MDA-MB-231 cells. However, CM from integrin  $\beta 4$ -overexpressing CAFs treated with the c-Jun inhibitor, sp600125, or the AMPK inhibitor, compound C, suppressed MDA-MB-231 cell growth (Figure 10B). These data demonstrate that integrin  $\beta 4$  expression in CAFs potentially plays a critical role in cancer cell proliferation by creating a tumor microenvironment replete with the high-energy metabolite – lactate, upon which cancer cells preferentially feed. We further examined MDA-MB-231 cell invasiveness, a commonly described histological characteristic of TNBC<sup>44</sup>. Our results indicate that cell invasiveness was significantly higher in MDA-MB-231 cells incubated with CM from integrin  $\beta 4$ -overexpressing CAFs in trans-well migration assays (Figure 10C). In contrast, CM from integrin  $\beta 4$ -overexpressing CAFs treated with sp600125 or compound C decreased the invasiveness of MDA-MB-231 cells (Figure 10C). Concomitantly, mRNA levels of epithelial-mesenchymal transition (EMT) inducer genes were also higher in MDA-MB-231 cells

stimulated with CM from integrin  $\beta$ 4-overexpressing CAFs, compared to both control MDA-MB-231 cells, and MDA-MB-231 cells stimulated with CM from integrin  $\beta$ 4-overexpressing CAFs that were treated with sp600125 or compound C (Figure 10D).

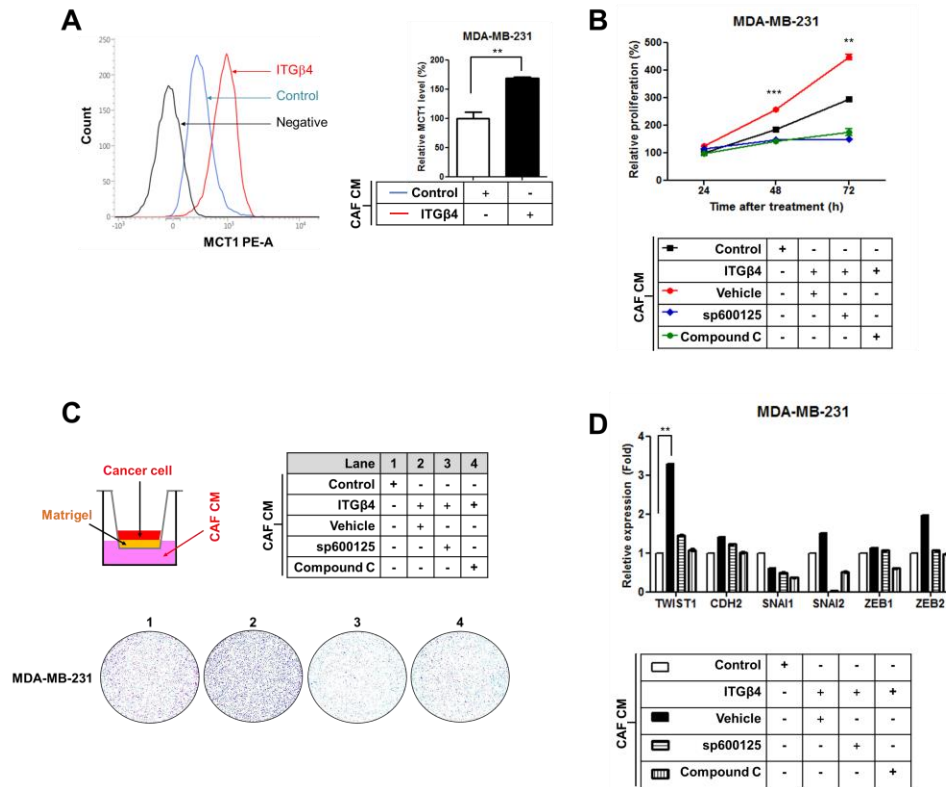


**Figure 10. Integrin  $\beta 4$ -dependent reverse Warburg effect contributes to breast cancer progression.** (A) The surface MCT1 level of TNBC cells stimulated by CM from integrin  $\beta 4$ -overexpressing CAFs. (B) The proliferation of TNBC cells stimulated by CM from integrin  $\beta 4$ -overexpressing CAFs and integrin  $\beta 4$ -overexpressing CAFs pretreated with sp600125 and Compound C. (C) The invasiveness of MDA-MB-231 cells was measured using matrigel invasion chamber. (D) The upregulation of EMT inducer expression was analyzed using real-time PCR. MDA-MB-231 cells were stimulated by CM from integrin  $\beta 4$ -overexpressing CAFs and integrin  $\beta 4$ -overexpressing CAFs pretreated with sp600125 and Compound C.

Immunohistochemical staining was performed to evaluate integrin  $\beta 4$  expression in CAFs in the xenograft. As expected, increased expression of integrin  $\beta 4$  was observed in CAFs injected with MDA-MB-231 (CAF+MDA-MB-231), compared to CAFs injected with integrin  $\beta 4$  knockdown MDA-MB-231 cells (CAF+shITG $\beta 4$ \_MDA-MB-231) (Figure 11A). In addition, CAF+MDA-MB-231 tumors were significantly larger compared to CAF+shITG $\beta 4$ \_MDA-MB-231 tumors (Figure 11B). Interestingly, we also found that CAF+MDA-MB-231 tumors developed blood vessels (Figure 11C) and further investigated angiogenesis in the tumors using immunohistochemical staining of CD31 and vascular endothelial growth factor (VEGF). Angiogenesis was induced in CAF+MDA-MB-231 tumors as demonstrated by increased staining of CD31 and VEGF (Figure 11C). The viability of immortalized CAFs in vivo was confirmed by fluorescence microscopy after scarifying mice (Supplementary Figure S2). Together, these data demonstrate that functional exosomal integrin  $\beta 4$  uptake by CAFs promote tumor growth and angiogenesis in TNBC.

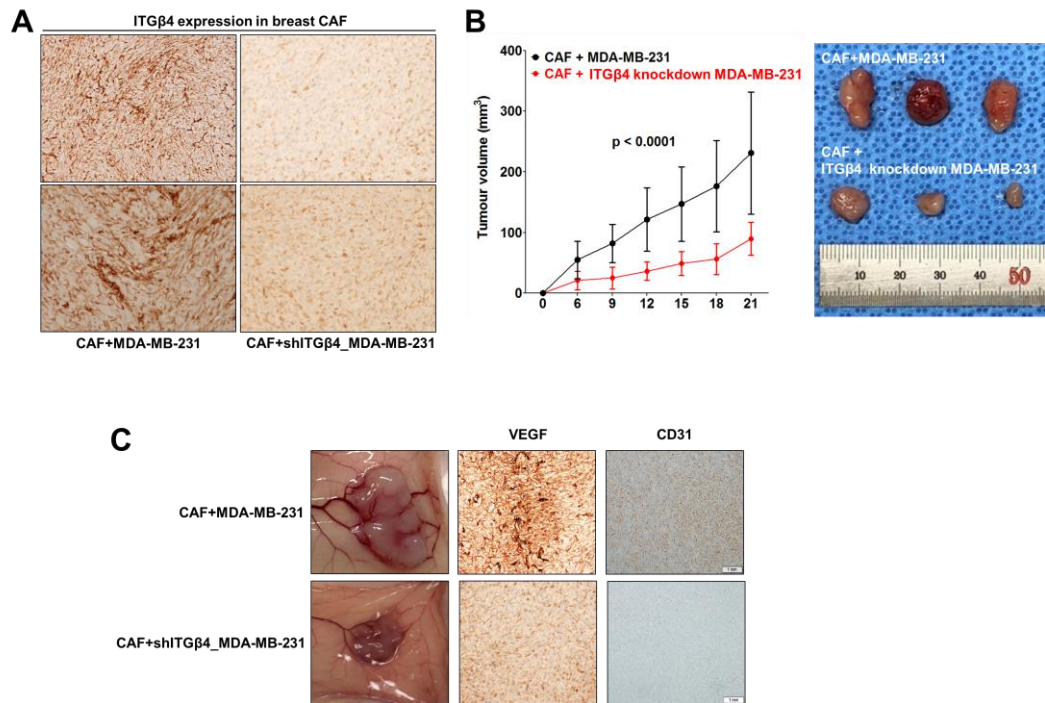


**Figure 11. Exosomal integrin  $\beta$ 4 promotes tumor growth and angiogenesis *in vivo*.** (A) Integrin  $\beta$ 4 overexpression in TNBC stroma using the mouse tumor tissues. Increased (C) tumor growth and (D) angiogenesis by integrin  $\beta$ 4-overexpressing CAFs in a mouse xenograft model. MDA-MB-231 or integrin  $\beta$ 4 knockdown MDA-MB-231 cells were subcutaneously co-transplanted with CAFs.

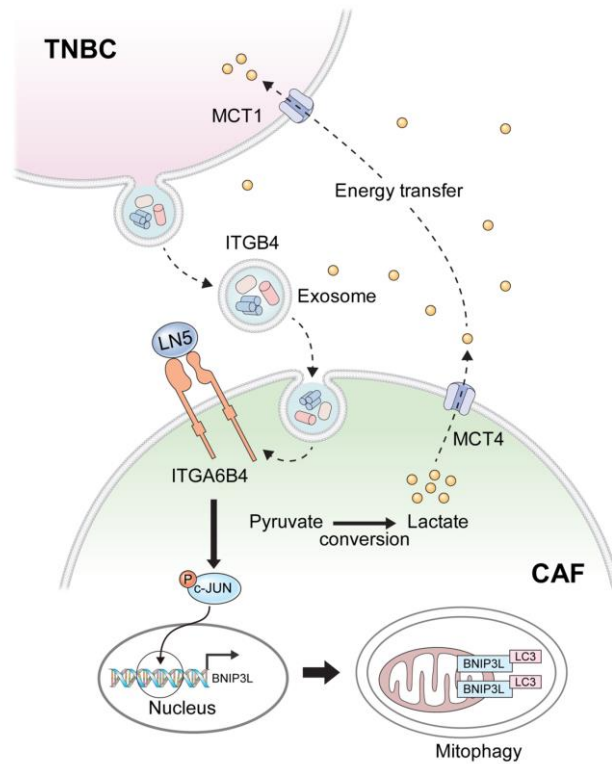
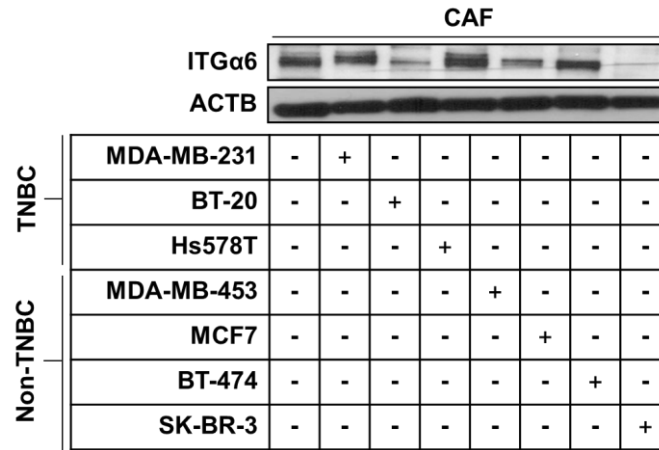
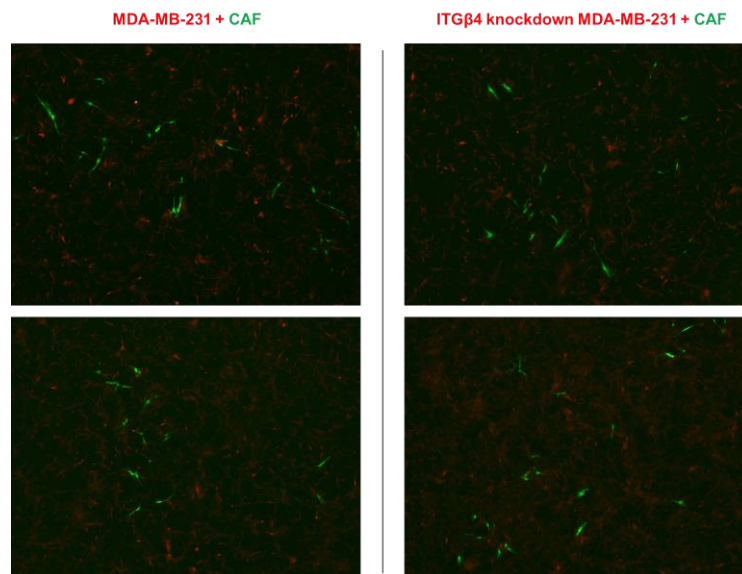


**Figure 12. Integrin  $\beta 4$ -mediated metabolic reprogramming of cancer-associated fibroblasts in triple negative breast cancer.** Integrin  $\beta 4$ -overexpressing TNBC cells provide CAFs with integrin  $\beta 4$  via exosomes. Once integrin  $\beta 4$  is transferred, integrin  $\alpha 6\beta 4$  is displayed on the surface of CAFs. LN5 (laminin-332) in extracellular microenvironment binds to the integrin  $\alpha 6\beta 4$ , and then initiates the mitochondrial expression of BNIP3L in CAFs via c-Jun phosphorylation. BNIP3L triggers mitophagy by binding with LC3, which results in the conversion of pyruvate to lactate in the CAFs. The produced lactates are exported from CAFs to extracellular microenvironment through MCT4, and then TNBC cells uptake them through MCT1.



**Supplementary Figure S1.** The expression of ITGα6 expression in the CAFs co-cultured with or without breast cancer cell lines.



**Supplementary Figure S2.** The fluorescence microscopic images of the mouse tumor tissues.

**Supplementary Table S1.** Primers for real-time PCR analysis.

Gene name	Strand	Sequence (5' to 3')	Annealing Tm (°C)
TWIST1	Forward	GTC CGC AGT CTT ACG AGG AG	53
	Reverse	CCA GCT TGA GGG TCT GAA TC	
SNAI1	Forward	TTT ACC TTC CAG CAG CCC TA	53
	Reverse	CCC ACT GTC CTC ATC TGA CA	
SNAI2	Forward	AAGCATTCAACGCCTCC AAA	54
	Reverse	GGATCTCTGGTTGTGGTATGACA	
ZEB1	Forward	TGC ACT GAG TGT GGA AAA GC	53
	Reverse	TGG TGA TGC TGA AAG AGA CG	
ZEB2	Forward	CGC TTG ACA TCA CTG AAG GA	53
	Reverse	CTT GCC ACA CTC TGT GCA TT	
CDH2	Forward	CTCCTATGAGTGGAACAGGAACG	53
	Reverse	TTGGATCAATGTCATAATCAAGTGCTGTA	
GAPDH	Forward	GTC AGT GGT GGA CCT GAC CT	52
	Reverse	TGC TGT AGC CAA ATT CGT TG	

## IV. DISCUSSION

Patients with TNBC have better response to chemotherapy than patients with other breast cancer subtypes<sup>45</sup>. This could be explained by the lack of therapeutic targets, leading to cause a high rate of fatality<sup>46</sup>. Personalized cancer therapy has been developed in the field of TNBC therapeutics for those who do not respond to chemotherapy. However, due to the heterogeneity of TNBC, recent studies propose the identification of a single targetable molecule in tumor microenvironment, imposing challenges for its treatment<sup>47-49</sup>.

Our study identified a novel function of integrin  $\beta 4$  in CAFs. Although integrin  $\beta 4$  is highly expressed in TNBC cell lines, only specific TNBC CAFs show its expression. Elevated integrin  $\beta 4$  expression accompanied with high levels of integrin  $\alpha 6$  and laminin-332, is associated with TNBC-specific integrin  $\beta 4$  expression in CAFs via exosomes. Considering that a laminin-332-rich tumor microenvironment is naturally established around TNBC and that integrin  $\alpha 6$  (the only pair partner) is intrinsically expressed at a high level in CAFs (Supplementary Figure S1). The role of integrin  $\beta 4$  is well-known to facilitate migration, invasion and survival of TNBC cells<sup>9-11</sup>. A recent study indicated that exosomal integrin  $\beta 4$  derived from breast cancer cells is involved in organotropic metastasis<sup>15</sup>. However, there has been little knowledge about the function of integrin  $\beta 4$  in CAFs. We showed that Increase in integrin  $\beta 4$  expression in CAFs up-regulated glycolysis and lactate production. These CAFs showed enhanced mitochondrial fission, possibly as a response to glycolytic stress.

Emerging studies have described that cleavage of Opa1 preventing further re-fusion of mitochondria facilitates the elimination of damaged mitochondria by mitophagy<sup>23-28,30-33</sup>.

In this study, induction BNIP3L suggested a significant increase in mitophagy upon integrin  $\beta$ 4 overexpression. c-Jun was identified as a transcription factor regulating BNIP3L gene expression activated by integrin  $\beta$ 4 in CAFs. BNIP3L is a key molecule that recruits the autophagic machinery<sup>35-39</sup>. Autophagy is promoted by AMPK followed by the overexpression of ULK1<sup>41-42</sup>. Integrin  $\beta$ 4-induced BNIP3L expression enhanced AMPK phosphorylation, and upregulated ULK1 and LC3 expression. Although integrin  $\beta$ 4 overexpressing CAFs showed an increase in autophagosome formation by entering autophagic pathway, they were not relevant for autophagic cell death. These observations suggest the potential role of integrin  $\beta$ 4 acquired by CAFs from TNBC-derived exosomes, leading to the production of excess lactate by controlling mitochondrial quality via mitophagy.

Lactate secreted by CAFs serves as a high-energy metabolite for adjacent TNBC cells. According to reverse Warburg effect, lactate is exported by MCT4 and imported by MCT1 in cancer cells, to be used as a fuel. In this study, MCT1 levels were elevated in TNBC cells grown in CM from integrin  $\beta$ 4-overexpressing CAFs, thus favoring TNBC cell proliferation and invasion. However, the detailed mechanism of this process remains unknown at this time. Our *in vivo* studies suggested the critical role of exosomal integrin

$\beta 4$  in tumor growth and angiogenesis, as integrin  $\beta 4$  knockdown in TNBC cells led to tumor suppression. Notably, the expressions of VEGF and CD31 were significantly upregulated in the presence of exosomal integrin  $\beta 4$  in the xenograft mouse model. We speculate that rapid tumor growth and angiogenesis of TNBC is mediated by exosomal integrin  $\beta 4$ -induced glycolysis in CAFs. Further studies are required to uncover the mechanisms by which TNBC cells are regulated by glycolytic CAFs. We predict that exosomal integrin  $\beta 4$  will emerge as an effective therapeutic target against TNBC.

## V. CONCLUSION

Here, we provide a novel function for the TNBC-specific expression of integrin  $\beta 4$  in CAFs. Integrin  $\beta 4$  is transferred to CAFs via exosomes derived from TNBC cells and promotes aerobic glycolysis. These glycolytic CAFs facilitate mitochondrial fission and mitophagy to maintain mitochondrial homeostasis. As CAFs elevate their lactate production, adjacent TNBC cells import lactate via MCT1 and utilize it as an energy source for cell proliferation, invasion, and angiogenesis. Together, these results represent a basis for TNBC development and further suggest that exosomal integrin  $\beta 4$  may be a potent therapeutic target against TNBC.

## REFERENCES

1. Conlin AK, Seidman AD. Taxanes in breast cancer: an update. *Curr Oncol Rep* 2007;9:22-30.
2. Curtis C, Shah SP, Chin SF, Turashvili G, Rueda OM, Dunning MJ, et al. The genomic and transcriptomic architecture of 2,000 breast tumours reveals novel subgroups. *Nature* 2012;486:346-52.
3. Malorni L, Shetty PB, De Angelis C, Hilsenbeck S, Rimawi MF, Elledge R, et al. Clinical and biologic features of triple-negative breast cancers in a large cohort of patients with long-term follow-up. *Breast Cancer Res Treat* 2012;136:795-804.
4. Kalluri R, Zeisberg M. Fibroblasts in cancer. *Nat Rev Cancer* 2006;6:392-401.
5. Howell A, Landberg G, Bergh J. Breast tumour stroma is a prognostic indicator and target for therapy. *Breast Cancer Res* 2009;11 Suppl 3:S16.
6. Finak G, Bertos N, Pepin F, Sadekova S, Souleimanova M, Zhao H, et al. Stromal gene expression predicts clinical outcome in breast cancer. *Nat Med* 2008;14:518-27.
7. Bianchini G, Qi Y, Alvarez RH, Iwamoto T, Coutant C, Ibrahim NK, et al. Molecular anatomy of breast cancer stroma and its prognostic value in estrogen receptor-positive and -negative cancers. *J Clin Oncol* 2010;28:4316-23.
8. Litjens SH, de Pereda JM, Sonnenberg A. Current insights into the formation and breakdown of hemidesmosomes. *Trends Cell Biol* 2006;16:376-83.

9. Stewart RL, O'Connor KL. Clinical significance of the integrin alpha6beta4 in human malignancies. *Lab Invest* 2015;95:976-86.
10. Guo W, Giancotti FG. Integrin signalling during tumour progression. *Nat Rev Mol Cell Biol* 2004;5:816-26.
11. Lipscomb EA, Mercurio AM. Mobilization and activation of a signaling competent alpha6beta4 integrin underlies its contribution to carcinoma progression. *Cancer Metastasis Rev* 2005;24:413-23.
12. Falcioni R, Sacchi A, Resau J, Kennel SJ. Monoclonal antibody to human carcinoma-associated protein complex: quantitation in normal and tumor tissue. *Cancer Res* 1988;48:816-21.
13. Koukoulis GK, Virtanen I, Korhonen M, Laitinen L, Quaranta V, Gould VE. Immunohistochemical localization of integrins in the normal, hyperplastic, and neoplastic breast. Correlations with their functions as receptors and cell adhesion molecules. *Am J Pathol* 1991;139:787-99.
14. Lu S, Simin K, Khan A, Mercurio AM. Analysis of integrin beta4 expression in human breast cancer: association with basal-like tumors and prognostic significance. *Clin Cancer Res* 2008;14:1050-8.
15. Hoshino A, Costa-Silva B, Shen TL, Rodrigues G, Hashimoto A, Tesic Mark M, et al. Tumour exosome integrins determine organotropic metastasis. *Nature* 2015;527:329-35.
16. Vlassov AV, Magdaleno S, Setterquist R, Conrad R. Exosomes: current knowledge of their composition, biological functions, and diagnostic and therapeutic potentials.

- Biochim Biophys Acta 2012;1820:940-8.
17. Pietras K, Ostman A. Hallmarks of cancer: interactions with the tumor stroma. *Exp Cell Res* 2010;316:1324-31.
  18. Cortez E, Roswall P, Pietras K. Functional subsets of mesenchymal cell types in the tumor microenvironment. *Semin Cancer Biol* 2014;25:3-9.
  19. Augsten M. Cancer-associated fibroblasts as another polarized cell type of the tumor microenvironment. *Front Oncol* 2014;4:62.
  20. Warburg O. On the origin of cancer cells. *Science* 1956;123:309-14.
  21. Semenza GL, Artemov D, Bedi A, Bhujwala Z, Chiles K, Feldser D, et al. 'The metabolism of tumours': 70 years later. *Novartis Found Symp* 2001;240:251-60; discussion 60-4.
  22. Pavlides S, Whitaker-Menezes D, Castello-Cros R, Flomenberg N, Witkiewicz AK, Frank PG, et al. The reverse Warburg effect: aerobic glycolysis in cancer associated fibroblasts and the tumor stroma. *Cell Cycle* 2009;8:3984-4001.
  23. Frank S, Gaume B, Bergmann-Leitner ES, Leitner WW, Robert EG, Catez F, et al. The role of dynamin-related protein 1, a mediator of mitochondrial fission, in apoptosis. *Dev Cell* 2001;1:515-25.
  24. Ishihara N, Jofuku A, Eura Y, Mihara K. Regulation of mitochondrial morphology by membrane potential, and DRP1-dependent division and FZO1-dependent fusion reaction in mammalian cells. *Biochem Biophys Res Commun* 2003;301:891-8.
  25. Montessuit S, Somasekharan SP, Terrones O, Lucken-Ardjomande S, Herzig S,

- Schwarzenbacher R, et al. Membrane remodeling induced by the dynamin-related protein Drp1 stimulates Bax oligomerization. *Cell* 2010;142:889-901.
26. Karbowski M, Lee YJ, Gaume B, Jeong SY, Frank S, Nechushtan A, et al. Spatial and temporal association of Bax with mitochondrial fission sites, Drp1, and Mfn2 during apoptosis. *J Cell Biol* 2002;159:931-8.
  27. Youle RJ, Karbowski M. Mitochondrial fission in apoptosis. *Nat Rev Mol Cell Biol* 2005;6:657-63.
  28. Fransson A, Ruusala A, Aspenstrom P. Atypical Rho GTPases have roles in mitochondrial homeostasis and apoptosis. *J Biol Chem* 2003;278:6495-502.
  29. Guido C, Whitaker-Menezes D, Capparelli C, Balliet R, Lin Z, Pestell RG, et al. Metabolic reprogramming of cancer-associated fibroblasts by TGF-beta drives tumor growth: connecting TGF-beta signaling with "Warburg-like" cancer metabolism and L-lactate production. *Cell Cycle* 2012;11:3019-35.
  30. Ehses S, Raschke I, Mancuso G, Bernacchia A, Geimer S, Tondera D, et al. Regulation of OPA1 processing and mitochondrial fusion by m-AAA protease isoenzymes and OMA1. *J Cell Biol* 2009;187:1023-36.
  31. Head B, Griparic L, Amiri M, Gandre-Babbe S, van der Blik AM. Inducible proteolytic inactivation of OPA1 mediated by the OMA1 protease in mammalian cells. *J Cell Biol* 2009;187:959-66.
  32. Mishra P, Carelli V, Manfredi G, Chan DC. Proteolytic cleavage of Opa1 stimulates mitochondrial inner membrane fusion and couples fusion to oxidative phosphorylation.

Cell Metab 2014;19:630-41.

33. Twig G, Elorza A, Molina AJ, Mohamed H, Wikstrom JD, Walzer G, et al. Fission and selective fusion govern mitochondrial segregation and elimination by autophagy. *EMBO J* 2008;27:433-46.
34. Gomes LC, Di Benedetto G, Scorrano L. During autophagy mitochondria elongate, are spared from degradation and sustain cell viability. *Nat Cell Biol* 2011;13:589-98.
35. Rambold AS, Kostecky B, Elia N, Lippincott-Schwartz J. Tubular network formation protects mitochondria from autophagosomal degradation during nutrient starvation. *Proc Natl Acad Sci U S A* 2011;108:10190-5.
36. Daido S, Kanzawa T, Yamamoto A, Takeuchi H, Kondo Y, Kondo S. Pivotal role of the cell death factor BNIP3 in ceramide-induced autophagic cell death in malignant glioma cells. *Cancer Res* 2004;64:4286-93.
37. Kanzawa T, Zhang L, Xiao L, Germano IM, Kondo Y, Kondo S. Arsenic trioxide induces autophagic cell death in malignant glioma cells by upregulation of mitochondrial cell death protein BNIP3. *Oncogene* 2005;24:980-91.
38. Hamacher-Brady A, Brady NR, Logue SE, Sayen MR, Jinno M, Kirshenbaum LA, et al. Response to myocardial ischemia/reperfusion injury involves Bnip3 and autophagy. *Cell Death Differ* 2007;14:146-57.
39. Tracy K, Dibling BC, Spike BT, Knabb JR, Schumacker P, Macleod KF. BNIP3 is an RB/E2F target gene required for hypoxia-induced autophagy. *Mol Cell Biol* 2007;27:6229-42.

40. Mammucari C, Milan G, Romanello V, Masiero E, Rudolf R, Del Piccolo P, et al. FoxO3 controls autophagy in skeletal muscle in vivo. *Cell Metab* 2007;6:458-71.
41. Egan DF, Shackelford DB, Mihaylova MM, Gelino S, Kohnz RA, Mair W, et al. Phosphorylation of ULK1 (hATG1) by AMP-activated protein kinase connects energy sensing to mitophagy. *Science* 2011;331:456-61.
42. Mack HI, Zheng B, Asara JM, Thomas SM. AMPK-dependent phosphorylation of ULK1 regulates ATG9 localization. *Autophagy* 2012;8:1197-214.
43. Maiuri MC, Le Toumelin G, Criollo A, Rain JC, Gautier F, Juin P, et al. Functional and physical interaction between Bcl-X(L) and a BH3-like domain in Beclin-1. *EMBO J* 2007;26:2527-39.
44. Weigelt B, Reis-Filho JS. Histological and molecular types of breast cancer: is there a unifying taxonomy? *Nat Rev Clin Oncol* 2009;6:718-30.
45. Carey, L. A, The triple negative paradox: primary tumor chemosensitivity of breast cancer subtypes. *Clin. Cancer Res.* 2007;13, 2329–2334.
46. Bonotto, M, Measures of outcome in metastatic breast cancer: insights from a real-world scenario. *Oncologist* 2014;19, 608–615.
47. Balko, J, Profiling of triple-negative breast cancers after neoadjuvant chemotherapy identifies targetable molecular alterations in the treatment-refractory residual disease. *Cancer Res* 2012;72, S3–S6.
48. Bauer, J. A, RNA interference (RNAi) screening approach identifies agents that enhance paclitaxel activity in breast cancer cells. *Breast Cancer Res* 2010;12, R41.

49. Balko, J. M, Profiling of residual breast cancers after neoadjuvant chemotherapy identifies DUSP4 deficiency as a mechanism of drug resistance. Nat. Med 2012;18, 1052–1059.

ABSTRACT (IN KOREAN)

삼중 음성 유방암 내 섬유아세포의 integrin  $\beta 4$  매개 신진대사 재구성

< 지도교수 조남훈 >

연세대학교 대학원 의과학과

성진솔

삼중 음성 유방암은 (TNBC)은 ER/PR/HER2가 모두 음성인 유방암으로 공격적인 특성을 보이며 재발률이 높고 유방암 중 가장 예후가 나쁜 것으로 알려져 있다. 현재까지 TNBC에 대해 효과가 입증된 표적 치료가 없어 새로운 치료 전략이 필요한 상황이다. 최근에는 종양 미세 환경을 표적으로 하는 새로운 치료전략이 주목을 받고 있다. 본 연구에서는 암세포의 주변 섬유아세포 (Cancer-associated fibroblast, CAF)에서 TNBC 특이적인 integrin  $\beta 4$ 의 발현이 엑소좀 (exosome)을 통해 CAF로 이동하는 것을 확인하였다. MDA-MB-231 세포에 exosome 분비를 억제 시켰을 때 CAF에서 integrin  $\beta 4$ 의 발현이 감소되었다. CAF에서의 integrin  $\beta 4$  발현은 젖산 생산과 해당 과정에 관여하는 유전자들의 발현을 증가시켰고, 이로 인한 당 분해 스트레스는 미토콘드리아의 분열과 미토콘드리아 기능유지를 위한 미토파지(mitophagy)를 증가시켰다. 또한 integrin  $\beta 4$

과발현된 CAF는 c-Jun의 활성화를 통해 미토파지에 관여하는 BCL2 interacting protein 3 like (BNIP3L) 발현을 증가시키는 것을 확인하였다. CAF에서의 integrin  $\beta$ 4 과발현은 microtubule associated protein 1 light chain (LC3)의 발현과 자가포식소체(autophagosome) 형성이 증가되었다. 또한 과량으로 생성된 젖산 증가는 monocarboxylate transporter 1 (MCT1)을 통해 TNBC세포의 성장(proliferation)과 침투(invasion)를 촉진시켰다. 이종이식 모델에서 exosome을 통해 CAF로 이동한 integrin  $\beta$ 4가 종양의 성장과 혈관생성을 증가시켰다. 종합적으로 본 연구에서는, exosome을 통한 CAF의 integrin  $\beta$ 4 발현이 과도한 젖산 생산을 증가시키고, TNBC 세포의 증식과 침투뿐만 아니라 종양의 성장과 혈관 생성을 촉진시키는 호기성 해당작용을 유도함을 확인하였다.

---

Key words : integrin  $\beta$ 4, 미토파지, 반대 윌버그 효과

## PUBLICATION LIST

1. **Sung JS**, Kang CW, Kang SK, Jang YS, Cho NH, Kim BG. ITGB4-mediated metabolic reprogramming of cancer-associated fibroblasts. *Oncogene*. 2019 Sep; doi:10.1038/s41388
2. Kim BG, **Sung JS**, Jang YS, Cha YJ, Kang SK, Han HH, Lee JH, Cho NH. Compression-induced expression of glycolysis genes in CAFs correlates with EMT and angiogenesis gene expression in breast cancer. *Communications Biology*. 2019 Aug; doi:10.1038/s42003